Multi-Feature Real Time Pedestrian Detection from Dense Stereo SORT-SGM Reconstructed Urban Traffic Scenarios

Ion Giosan and Sergiu Nedevschi
Computer Science Department, Technical University of Cluj-Napoca, Romania
{Ion.Giosan, Sergiu.Nedevschi}@cs.utcluj.ro

Keywords: Driving Assistance Systems, Dense Stereo, SORT-SGM, Multi Features, Pedestrian Detection

Abstract: In this paper, a real-time system for pedestrian detection in traffic scenes is proposed. It takes the advantage of having a pair of stereo video-cameras for acquiring the image frames and uses a sub-pixel level optimized semi-global matching (SORT-SGM) based stereo reconstruction for computing the dense 3D points map with high accuracy. A multiple paradigm detection module considering 2D, 3D and optical flow information is used for segmenting the candidate obstacles from the scene background. Novel features like texture dissimilarity, humans' body specific features, distance related measures and speed are introduced and combined in a feature vector with traditional features like HoG score, template matching contour score and dimensions. A random forest (RF) classifier is trained and then applied in each frame for distinguishing the pedestrians from other obstacles based on the feature vector. A k-NN algorithm on the classification results over the last frames is applied for improving the accuracy and stability of the tracked obstacles. Finally, two comparisons are made: first between the classification results obtained by using the new SORT-SGM and the older local matching approach for stereo reconstruction and the second by comparing the different features RF classification results with other classifiers' results.

1. INTRODUCTION

Nowadays, building intelligent vehicles is a challenge for both the researchers and the vehicle constructors. In such vehicles with driving assistance systems on board, an important aspect is related to the obstacles detection, tracking and classification.

Pedestrians are the most vulnerable participants involved in traffic. Distinguishing the pedestrians from the other traffic obstacles (Dollar et al., 2012) is obviously very important for protecting them by alerting the driver in case of a dangerous situation. In other case of an imminent impact, if the vehicle has special protection artifacts they should be automatically triggered, for example a special external airbag of the vehicle is opened to attenuate the impact with the pedestrian.

The main objective is to reliably detect pedestrians and after that to protect them. The false positive rate should be very low in order not to cause false alarms to the driver nor falsely trigger the vehicle's protection parts. Finding the pedestrians that appear in the traffic scenarios is a requirement that almost every safety driving assistance system must have.

Pedestrian detection is a very simple problem for humans but it is a complex one for driving assistance systems due to the large variations of pedestrians body poses, clothing, accessories which they are carrying and due to the variations of background scene, the environment conditions, the distance to the acquisition cameras and their resolution, the unpredictable vibrations of the intelligent vehicle and scene cluttering. An important aspect is that the pedestrian detection should be done in real time and this aspect makes the detection a very complex process which needs many efficient and robust algorithms.

Driving assistance systems may be used in different traffic scenarios. In highway scenarios, the scene is relatively simple, the pedestrians are almost missing and the obstacles that appear in the traffic are limited to cars, trucks, poles and road-side fences. An opposite scenario is the urban traffic where the pedestrian detection problem becomes much more difficult due to the environment complexity and the presence of different objects types.

There are many different technologies (Gandhi and Trivedi, 2006) such as LIDAR, RADAR, ultra-sound sensors, infrared sensors (Fardi et al., 2005), LASER-scanners, piezo-electrical sensors and mono (Dollar et al., 2012), color, stereo (Keller et al., 2011b) cameras (Gavrila et al., 2004) that are widely used for acquiring the traffic environment information. However, the images acquired with video cameras have rich information and it's a passive and clean way because it doesn't affect the environment or people and doesn't imply any source of pollution.

Due to the fact that the urban traffic scenarios are very complex with many kinds of obstacles, we choose a stereo-vision sensor for scene images acquisition. The stereo sensor offers us the possibility to accurately determine the depth distance value for the scene points and further to assign motion vectors to them. The SORT-SGM stereo reconstruction (Pantilie and Nedevschi, 2012) implemented on GPU has the advantage of providing a dense stereo depth map with high accuracy in a short processing time. The depth map is denser and more accurate than the one obtained with a local matching technique implemented on a classic hardware stereo-machine (Woodlill et al., 2004). Using both accurate 3D pixels positions and their associated optical flow motion information significantly improves localization and representation of scene obstacles which finally leads to a better classification of pedestrians or other obstacles.

We present a complete solution for pedestrian detection system starting from images acquisition, 3D points' computation, obstacles detection and tracking, novel and accurate features extraction due to the stereo reconstruction and ending with the classification of obstacles in pedestrians or non-pedestrians.

A first comparison is made between the classification results obtained by using the SORT-SGM GPU implementation algorithm and a hardware local matching approach for stereo reconstruction. The second one compares the RF classification results with other classifiers' results. We emphasize the better RF classification results obtained when considering the SORT-SGM reconstructed obstacles.

2. RELATED WORK

A lot of research work has been performed for developing smart modules used in driving assistance systems or surveillance applications for robust pedestrian tracking and classification. Basically, the general architecture of a stereovision pedestrian detection system (Nedevschi et al., 2007) consists of the following three main modules: candidates (obstacles) detection and localization (Llorca et al., 2012) based on 3D points grouping (Pocol et al., 2007) and density maps (Nedevschi et al., 2009); motion detection and candidates tracking (Danescu et al., 2007), (Bota and Nedevschi, 2011a); candidates classification in pedestrians and other classes (Bota et al., 2009).

In 2D image space, each scene obstacle could be represented as a set of blobs. This model has the disadvantage that the entire obstacle bounding box that is formed by combining all the blobs may be wrongly defined due to common occlusions and can also lead to erroneous tracking across a sequence of frames. In this manner, the candidate pedestrians' parameters estimation using a Kalman filter is described in (Masoud and Papanikolopoulos, 2001). The 3D geometry of a moving obstacle may partially solve the occlusion issue, but it has the disadvantage that it is very time consuming so it can't be used in case of detailed geometric obstacle models. In (Koller et al., 1993) the issue of partial obstacle occlusion is solved by computing their corresponding 3D models. A quadratic unconstrained binary optimization (QUBO) framework for reasoning about multiple object detections with spatial overlaps may also be used in order to solve the pedestrian detection occlusion problem (Rujikietgumjorn and Collins, 2013).

Computing the motion correspondence for each obstacle is also important (Javed and Shah, 2002). The obstacle's size and position is used with Kalman predictors (Stauffer and Grimson, 2000) in order to correctly estimate as much as possible its real trajectory. In case that the objects types are pedestrians a set of appearance models representing body-silhouettes can be used for their tracking (Haritaoglu et al., 2000). Probabilistic objects appearance models were used as well in (Elgammal et al., 2002) for pedestrian detection and tracking. Probabilistic tracking approaches (Bregler, 1997) decompose the pedestrians' motion in video sequences in order to learn and recognize their attitudes. A simple tracking (Lipton et al., 1998) based both on temporal differencing and image template matching is used. It has high tracking performance in case of partial occlusions presence and it achieves also a good classification.

Different approaches are proposed in literature for pedestrian detection but the problem of achieving an accurate and robust classification in complex traffic scenarios is still far from being solved. Usually, a set of discriminant features are considered for classifying the obstacles in pedestrians and non-pedestrians.

The obstacle contour is a good feature for pedestrian detection (Hilario et al., 2005) because it eliminates most of the issues, briefly presented in the introduction, which could lead to weak detection (high false positive and false negative rates). The contour clearly describes the shape of the obstacle and it is invariant for pedestrians' clothing variety and scene illumination. Scene obstacles are usually matched against a set of pedestrian contour templates in order to determine if they are pedestrians or not. A method for pedestrian detection using a pattern matching with a hierarchy of contour templates is presented in (Gavrila and Philomin, 1999). Pedestrian detection based on shapes and edges, using monocular vision is described in (Broggi et al., 2000). A hierarchy of pedestrian contours reduces the search space, achieving a real-time matching process between the pedestrian candidate contour and the pedestrian contours templates. Such pedestrian detection systems using contour templates are proposed in (Gavrila, 2000), (Gavrila and Munder, 2007) and (Nedevschi et al., 2009).

A pedestrian detection method based on local multi-scale oriented gray-levels differences, obtained by computing the Haar wavelet transform and using a SVM classifier is described in (Papageorgiou and Poggio, 2000). A robust and complete pedestrian detection system that uses stereo depth segmentation, shape chamfer matching, neural networks for texture classification and stereo-based tracking and verification is presented in (Gavrila et al., 2004).

Shape structural extraction and tracking, like the legs and their symmetry detection using morphological operators are used for pedestrian detection and described in (Havasi et al., 2004). In (Hilario et al., 2005) an active contours approach is used for pedestrian segmentation and stereovision for guiding the active contour to its appropriate location.

Pattern matching pedestrian detection method is limited to the image intensity information (Gavrila, 2000). Other features classification approaches such as Adaboost classifiers are also widely used for achieving an improvement in the pedestrian detection (Khammari et al., 2005). Gray-levels features are also used for the detection of image regions having a significant amount of vertical edges (Broggi et al., 2000). They are considered as being pedestrian candidates regions used further in the obstacle classification process.

Many algorithms for obstacle classification including pedestrians are proposed in literature, but the problem of achieving a very good classification result that can be successfully used in driving assistance systems in complex traffic urban scenarios is still far from being solved. In (Toth and Aach, 2003) a feed-forward neural network is used for distinguishing between vehicles, pedestrians, and other background obstacles. SVM (Rivlin et al., 2002) may also be used for pedestrians, vehicles and animals classification. Another classifier using error correction output is presented in (Lun et al., 2007) and used for classification of cars, trucks, bikes, pedestrians and groups of pedestrians. In (Javed and Shah, 2002) a classifier that doesn't need to be trained with different obstacles is well used for classification. In modeling the traffic environment, we considered four main types of obstacles: pedestrians, cars, poles and other objects.

Two algorithmic speed-ups, one for monocular images and the other for stereo images achieve pedestrian detections at 100 fps with very high detection quality (Benenson et al., 2012). A pedestrian detection benchmark from stereo images with an evaluation methodology are described in (Keller et al., 2011a). The benefits of stereovision for ROI generation and localization are also quantified.

Usually, the stereo-information comes to enrich the image intensity information for achieving a robust pedestrian detection. The dense stereo reconstruction information obtained from local matching methods is still noisy and has lower confidence than intensity data. In (Gavrila et al., 2004), a system used for pedestrian detection uses the 3D information just for validating the classification results. The SORT-SGM dense stereo reconstruction (Haller and Nedevschi, 2010) offers a higher accuracy of the 3D pixels information, so it leads to accurate features extraction for obstacles which determines a better pedestrian detection.

Multiple novel discriminant obstacle features are extracted in order to train a classifier that detects the pedestrians from the entire scene obstacle set. The classifier is applied individually at each frame. Unfortunately, the classification algorithms are not powerful enough to accurately predict the obstacles' classes (pedestrians vs. other obstacles) considering just the current frame. A robust classification tracking technique is used in order to achieve better classification results across a sequence of frames.

3. PEDESTRIAN DETECTION

In this chapter, the entire architecture of the pedestrian detection system, from image acquisition to final classification, together with a briefly description of each module input data, implemented algorithms and output data is presented.

3.1 System Architecture

The pedestrian detection system architecture with all its component modules and data flow is depicted in Figure 1.

A driving assistance system based on computer vision data processing which integrates a pedestrian collision module is generally classified by the cameras field of view, angular resolution, detection range, range resolution, illumination type, algorithmic complexity and hardware cost (Gandhi and Trivedi, 2006).

The stereo-cameras images acquisition system has wide field of view of about 68 degrees, with medium angular resolution at 8 minutes of arc, medium detection range at about 25m, as it is very difficult to detect pedestrians beyond this distance, due to the wide field of view we use. The range resolution is high by taking advantage of 3D information (2D grayscale left and right camera images plus the depth information that is computed with a stereo-matching algorithm rather than simply inferred from a single monocular image) and a high precision calibration procedure (Marita et al., 2006).

No active illumination techniques are used, which we consider to be an advantage. Normal gray levels cameras are used which lead to a medium hardware cost. The entire acquisition system is mounted inside a demonstrator vehicle.

Gray levels images, left and right cameras images (with 512x383 pixels) of the traffic scene are acquired with the above mentioned stereo vision system.

An improved sub-pixel semi-global matching method with Census transform as the matching method is used in order to compute high accuracy dense stereo reconstruction of the scene considering the two input gray-levels images (Haller and Nedevschi, 2010). NVIDIA GeForce GTX 580 video card and a corresponding parallel implementation on the GPU offer us the possibility of executing this complex algorithm in real time obtaining high-accuracy results at sub-pixel. Figure 2 depicts a comparison between this approach and an older one, that uses a hardware stereo machine (TYZX) (Woodlill et al., 2004) with local matching method for computing the depth map. In the depth map each scene point encodes the distance from the stereo pair of cameras, resulting a 3D set of points (2D intensity levels and their corresponding distances).

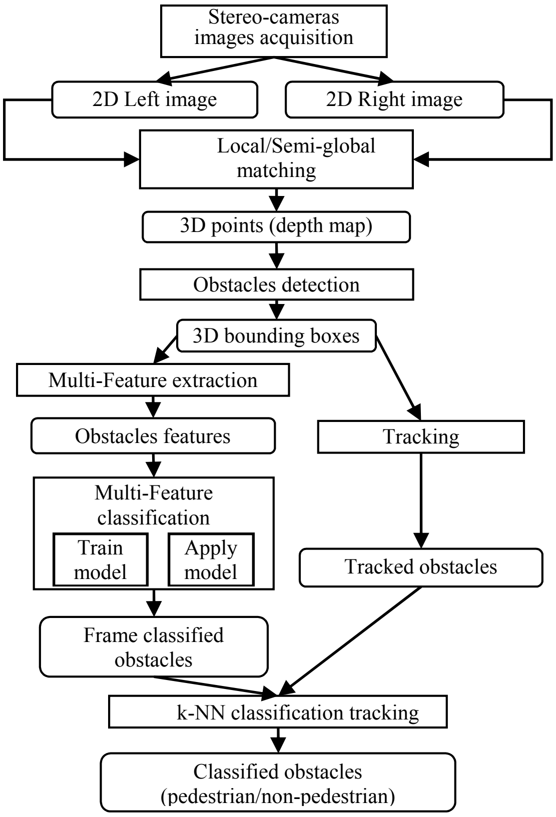
Stereo-cameras images acquisition
2D Left image
2D Right image
Local/Semi-global matching
3D points (depth map)
Obstacles detection
3D bounding boxes
Multi-Feature extraction
Obstacles features
Tracking
Multi-Feature classification
Train model
Apply model
Tracked obstacles
Frame classified obstacles
k-NN classification tracking
Classified obstacles (pedestrian/non-pedestrian)

Figure 1: Pedestrian detection system architecture

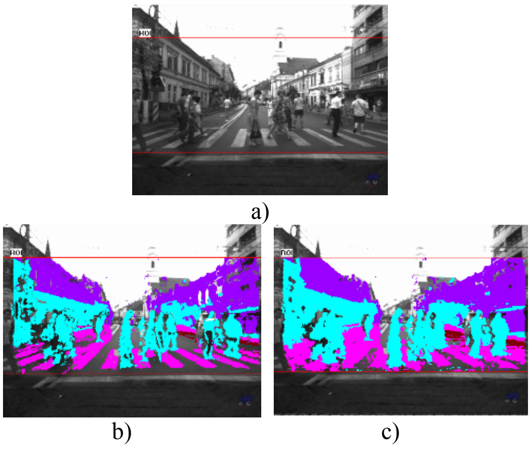

Figure 2: a) Example of a grayscale image acquired with left camera; b) reconstructed points with TYZX; c) reconstructed points with SORT-SGM on GPU

In the reconstruction example shown in Figure 2 there is a significant improvement in the number of scene stereo-reconstructed points: about 61000 points obtained with TYZX and about 77000 points with the GPU semi-global matching implementation.

Generally, we notice an increase of the 3D points number with almost 25%.

First step in obstacles detection consist in separating the foreground points (obstacle points) from those belonging to the road or background. In Figure 3 we notice that the computed foreground 3D points situated on the obstacle (in this case a pedestrian) are better obtained in case of using the SORT-SGM GPU reconstruction instead of a TYZX local matching approach.

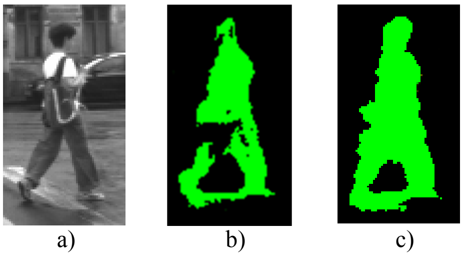

Figure 3: a) A pedestrian closer view in 2D left image; b) pedestrian's 3D points with TYZX local; c) pedestrian's 3D points with GPU SORT-SGM

Second step of the detection algorithm is applied on the previously computed depth map in order to find and fit the 3D bounding boxes (oriented cuboidal model) on all obstacles from the scene image.

A multi-paradigm based on both vicinity of the 3D points which determine the occupied areas (Pocol et al., 2007) and density maps (Nedevschi et al., 2009) is used for computing the obstacles 3D oriented bounding box. A set of segmented obstacles is shown in Figure 4.

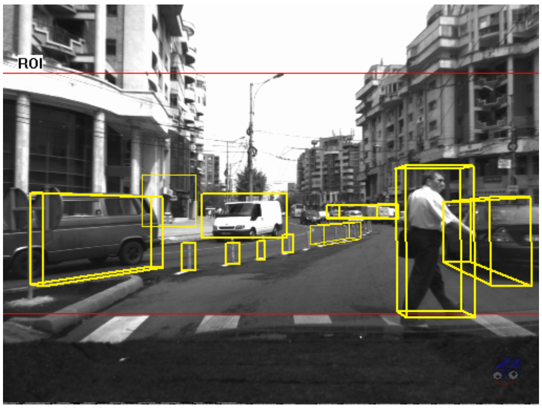

Figure 4: Urban traffic obstacles bounding boxes obtained from stereo-reconstructed points

An obstacle tracking algorithm (Bota and Nedevschi, 2011b), based on dense stereo obstacle points and optical flow information is then used. It defines a probabilistic cuboidal model for objects and uses a dynamic model differently adapted to each class of obstacles. It deals with hierarchical objects and the results shows that the tracking algorithm improves the performance of obstacle detection module.

3.2 Multi-Feature Extraction

In order to distinguish between pedestrians and all the other obstacle classes that were considered (cars, poles and other objects) we extract a vector of features FV – equation (1) – based on both depth and gray-levels information. In the following, all the relevant features extracted in the feature vector are briefly described and their distribution across classes is depicted (color-class assignment is shown in Figure 8).

$$FV = \left(H, W, L, PM, TD, HS, SX, SZ, AR, AC, HR, HC\right) \tag{1}$$

Due to the accurate stereo-reconstruction, the obstacles dimensions, contours, surfaces, projections are much more accurate and determine a feature vector with accurate values closer to the ground truth.

3.2.1 Obstacles Dimensions

The 3D bounding box obstacle dimensions (height H, width W, length L) are firstly inserted in the feature vector. We notice that the height feature distinguishes cars and pedestrians from other classes while width and length feature distinguish pedestrians, poles and other obstacles from cars. An obstacle is considered to be a pedestrian hypothesis only if it has specific dimensions: height in range of 1m to 2m; width in range of 0.25m to 1m; aspect ratio (height/width) in range of 1 to 4.

3.2.2 Template Pattern Matching Score

A novel pattern matching score PM (4) is computed for every pedestrians hypothesis (Giosan et al., 2009). A full body contour extraction algorithm is applied on the projected foreground points of each candidate pedestrian (Figure 3), resulting an exterior continuous contour for that obstacle (Figure 7). The matching is done between this contour and a hierarchy H containing about N=1900 pedestrian contour templates. The hierarchy is a multi-way tree (Giosan and Nedevschi, 2009).

The matching process has two phases. First is a contour-to-template matching: the contour C of the hypothesis is superimposed on the templates T in the pedestrian contour hierarchy. A Distance Transform (DT) is applied on the template contour. A score PM_{CT} – equation (2) – is computed by summing the pixels intensities (distances) in the template contour DT image that lie below the contour hypothesis. Second is a template-to-contour matching which is similar to the first step and computes another score PM_{TC} – equation (3). The pattern matching score PM – equation (4) – is considered as being the maximum between those two scores. The lower the pattern matching score, the higher is the probability for an obstacle to be detected as being a pedestrian.

$$PM_{CT_i} = \text{Match}\left(C, DT\left(H\left(T_i\right)\right)\right) \tag{2}$$

$$PM_{T_iC} = \text{Match}\left(H\left(T_i\right), DT\left(C\right)\right) \tag{3}$$

$$PM = \underset{i=1,N}{\text{TreeSearchMin}}\left(\text{Max}\left(PM_{TiC}, PM_{CTi}\right)\right) \tag{4}$$

It is clear that having an accurate sub-pixel semi-global stereo-reconstruction algorithm (Figure 3b) leads to a better fitting of the foreground points' exterior contour to the real shape contour of the obstacle and a more precise matching score.

3.2.3 Texture Dissimilarity Score

The new texture dissimilarity score TD – equation (5) – measures the maximum vertical dissimilarity that can be found in the obstacle's area. It is computed considering a part of the 2D object image which represents the middle vertical area of the object. The projected 2D image coordinates of the obstacle's center of mass are computed by keeping only the obstacle points (foreground points). The texture analysis ROI considered (R) is the rectangular area having 1/3 of the object 2D image in width, the whole height of the 2D image, and it is centered in the horizontal position of the center of mass.

A set of vertical displacements V (1 to 5 pixels) is considered to compute the gray level co-occurrence matrix (Figure 5). The vertical texture dissimilarity coefficient is computed for each vertical displacement as being the average of the weighted difference of intensities I from the co-occurrence matrix. Finally the vertical texture dissimilarity is set to the maximum of the previously computed coefficients.

$$TD = \max_{v=1,5}\left(TD_v\right) \tag{5}$$

$$TD_v = \underset{\substack{(i,j)\in R,\\ (i+v,j)\in R}}{\text{avg}}\left(\left|I\left(i,j\right) - I\left(i+v,j\right)\right|\right) \tag{6}$$

The vertical texture dissimilarity has high values for pedestrians due to their clothing and low values for trees/poles due to their homogenous aspect. This feature is successfully used for distinguishing between pedestrians and poles/trees.

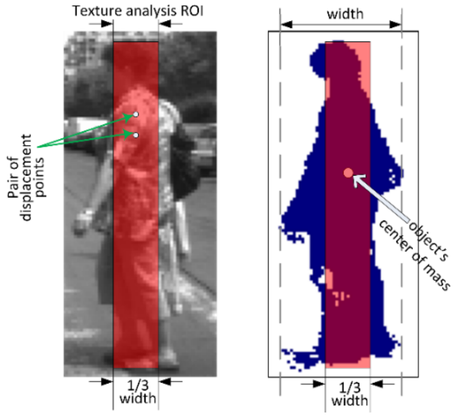

Figure 5: Texture analysis: a) ROI with its position, size and an example of a pair of displacement points used for co-occurrence computations; b) depth mask

The score has high values for pedestrians due to their textured clothing and low values for poles due to their homogenous aspect. It is used for distinguishing between pedestrians and poles/trees.

3.2.4 HoG Score

The HoG score HS is given by a set of trained boosted classifiers. They operate on the 2D image and for each obstacle hypothesis by computing the histogram of oriented gradients (HoG) (Dalal and Triggs, 2005). The HoG features are obtained by dividing the 2D image corresponding to the projected 3D cuboid surrounding the object, into non-overlapping cells of equal dimension. A weighted histogram of orientations is built within each cell. The cells are then grouped in overlapping blocks and the values of the histograms contained by a block are normalized. A positive training set of pedestrians and negative samples regions from images containing other obstacles (Figure 6) are used in order to train a cascade of boosted classifiers. These classifiers offers a prediction score which represents the value of the HoG score in our feature vector.

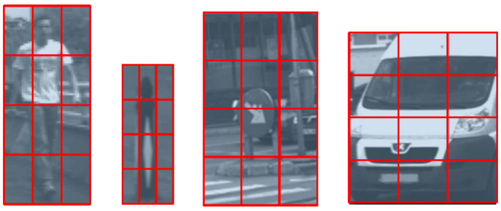

Figure 6: Intensity images with pedestrian and other obstacles divided in equal dimension cells used for HoG computation

3.2.5 Speed

The lateral speed (*SX*) and longitudinal speed (*SZ*) are extracted for all kinds of obstacles using the obstacle tracking module. They are less discriminant, except the longitudinal speed that sometimes can distinguish the pedestrians from moving cars and other obstacles.

3.2.6 Distance and Surface Related Measures

Novel features like area-root-distance *AR* – equation (7) –and area-cube-distance *AC* – equation (8) – are computed by multiplying the obstacles' projection area P_A (expressed in pixels) into the left image with the square root of its distance (*D*) from the cameras and respectively with the cubic distance (expressed in millimeters).

$$AR = P_A \sqrt{D} \qquad (7)$$

$$AC = P_A D^3 \qquad (8)$$

3.2.7 Humans' Body Specific Features

Two features based on the upper part of the obstacles are extracted. Usually the head of a human is 1/7 height of the entire body. We model that 1/7 upper part as an ellipse and the rest of the body with a rectangle (Figure 7c). The head-to-rest-body ratio score *HR* – equation (9) – is obtained by dividing the transverse diameter *td* of the ellipse with the width of the rectangle *rw*. The other feature refers to the head circularity *HC* – equation (10) – which clearly separates the pedestrians from other classes. The circularity is computed as being the thinness ratio of the upper 1/7 region of the pedestrian.

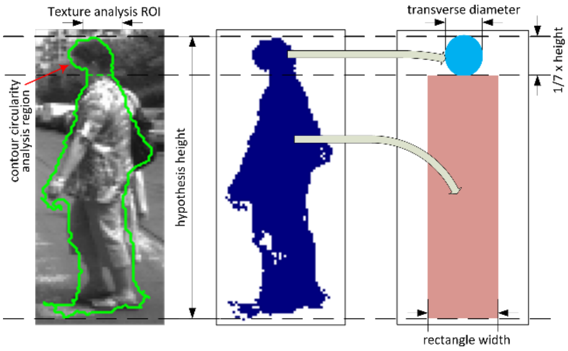

a) b) c)

Figure 7: Pedestrian measures: a) intensity image with full body contour and the ROI for contour circularity analysis; b) depth mask; c) dimensions for modeling the head with an ellipse and the body with a rectangle

$$HR = \frac{td}{rw} = \frac{24}{\pi} \cdot \frac{Area_{Head}}{Area_{RestOfBody}} \qquad (9)$$

$$HC = 4\pi \frac{Area_{Head}}{Perimeter_{Head}^{\;2}} \qquad (10)$$

3.3 Multi-Feature Classification

In order to train a classifier, we extracted the feature vector for a large set of obstacles with known corresponding class (obtained through a manual labeling procedure). A random forest classifier, based on the dataset's feature vectors, is built using the WEKA machine learning tool.

We considered equal numbers of pedestrians and other classes' instances for classifier training (Figure 8). Among other traditional classifiers like AdaBoost, J48 trees, multilayer perceptron, the random forest has the advantages of no need for pruning trees, accuracy and variable importance generated automatically, no overfitting, not sensitive to outliers and missing data. The result is a random-forest classifier model. This model is applied, frame by frame, on the entire set of hypotheses contained in that frame.

The classification pedestrian/non-pedestrian result isn't stable across frames. The feature vector used in the classifier input for the same object is changing from frame to frame. A k-NN classification on the computed class values over the last few frames is applied for improving the accuracy and stability of the tracked obstacles across multiple frames. We assume that the pedestrian hypothesis is right classified in almost all frames where it is tracked, but there are few frames where the classification gets a wrong result. The objective is to filter these wrong classifications and modify them to the right class. The k-NN method is suitable for accomplishing this task. Considering the value *k* as being the number of last frames where the object appeared in its tracks, and knowing the class W_f that is assigned for the object at frame *f*, we vote for each class appearance in all *k* frames.

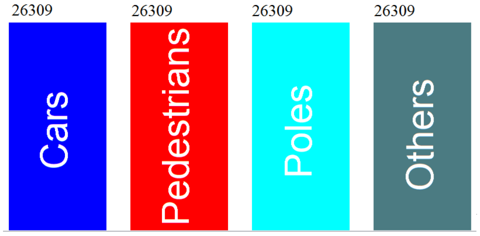

Figure 8: Uniform distribution of instances used for building the classification model

$$C = \{Pedestrian, NonPedestrian\}$$

$$V(C_i) = \sum_{f=1}^{k} W_f(C_i),\ i = 1,2 \quad (11)$$

$$W_f(C_i) = \begin{Bmatrix} 1,\ if\ hypotesis\ class\ is\ C_i\ in\ frame\ f \\ 0,\ otherwise \end{Bmatrix}$$

After computing all the votes in the last *k* frames with equation (11), the hypothesis class index is reassigned in current frame as being that class having the maximum number of votes – equation (12).

$$W = \underset{i=1,2}{\arg\max}\left(V(C_i)\right) \quad (12)$$

4. EXPERIMENTAL RESULTS

In this chapter we present the pedestrian detection results achieved using the features and the classification model previously described. All the proposed algorithms were tested on sequences of grayscale images with thousands of frames from different traffic scenarios acquired with our stereo-vision cameras system.

We have built a large database containing about 100000 obstacles (pedestrians, cars, poles, other objects) together with their feature vector and their class (assigned by manual labeling). The distribution of all four classes is uniform (Figure 8).

The features distributions among classes are depicted in Figure 9 (the class corresponding colors are shown in Figure 8). There are features that are weak discriminant between pedestrians and non-pedestrians, but their contribution to the final classification is significant. The most relevant features are: obstacle dimensions, pattern matching score, HoG score, texture dissimilarity, head-to-rest-body and head circularity.

A comparative analysis about how the pedestrian detection is affected by the dense stereo reconstruction was done. We considered the TYZX local matching reconstruction against SORT-SGM GPU software implementation for computing the depth of each scene point.

A random forest classifier with a number of *k* random trees was trained for classifying the obstacles (pedestrians/non-pedestrians). The trees' depth is unlimited and a random selection of features is used to split each node. A number of $\log_2(TNA)+1$ attributes was used in random selection, where *TNA*=12 represents the total number of attributes from the feature vector. The value of *k* was found by analyzing the ROC curve (Figure 10) among a set of experimental values. The value *k*=30 seems to achieve good results, generating a fast non-oversized classifier model.

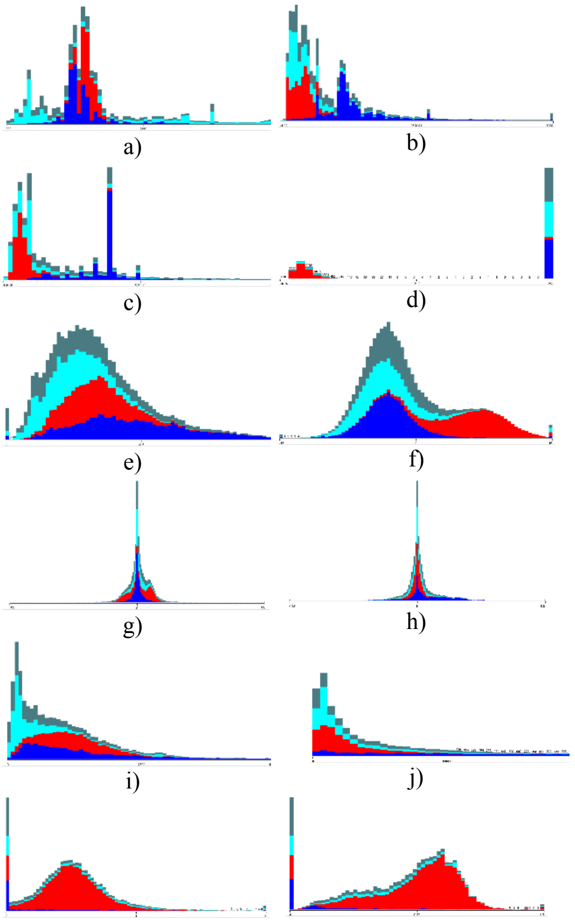
a)
b)
c)
d)
e)
f)
g)
h)
i)
j)
k)
l)

Figure 9: Obstacle classes feature distributions (pedestrians vs. poles, cars and others objects): a) height; b) width; c) length; d) pattern matching score; e) texture dissimilarity score; f) HoG score; g) lateral speed; h) longitudinal speed; i) area-root-distance; j) area-cube distance; k) head-to-rest-body ratio; l) head circularity

The advantage of the novel proposed features is proven by experimenting the obstacles classification with and without these features. Better results are obtained with novel features (Table 1) than without them (Table 2).

Multiple classifiers were considered in order to emphasize the benefits of the random forest classifier in this task. A comparison between the pedestrian detection results obtained with random forest and other classifiers like J48 trees, AdaBoostM1, multilayer perceptron, RBF network is presented in Table 3.

Table 1: Pedestrian detection results with novel features

	TYZX local matching stereo reconstruction		SORT-SGM stereo reconstruction	
k	FP rate	TP rate	FP rate	TP rate
5	0.049	0.934	0.035	0.940
10	0.040	0.942	0.033	0.945
20	0.034	0.950	0.025	0.951
30	0.030	0.953	0.022	0.955
50	0.030	0.956	0.022	0.956

Table 2: Pedestrian detection results without novel features

	TYZX local matching stereo reconstruction		SORT-SGM stereo reconstruction	
k	FP rate	TP rate	FP rate	TP rate
5	0.064	0.913	0.051	0.920
10	0.059	0.923	0.050	0.930
20	0.051	0.933	0.042	0.936
30	0.048	0.938	0.040	0.941
50	0.048	0.940	0.040	0.942

Table 3: Random Forest vs. other classifiers results

Classifier	Pedestrian detection (SORT-SGM stereo reconstruction)	
	FP rate	TP rate
J48 trees	0.032	0.927
AdaBoostM1	0.084	0.932
Mutilayer perceptron	0.033	0.933
RBF network	0.036	0.891
Random forest (k=30)	0.022	0.955

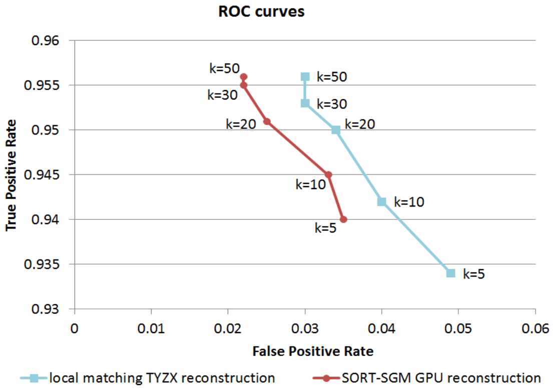

Figure 10: Pedestrian detection ROC curves: local matching reconstructed points vs. SORT-SGM reconstructed points

We evaluate the classifier using a stratified cross validation with 10 folds. Statistically, using the SORT-SGM instead of the local matching approach and the proposed novel features, the pedestrian detection was improved by about 2.6% in false

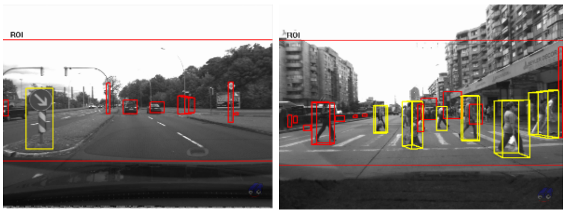

Figure 11: Samples obstacle misclassifications solved by SORT-SGM (pedestrians with yellow color; other obstacles with red color): left image – a false positive; right image – a false negative

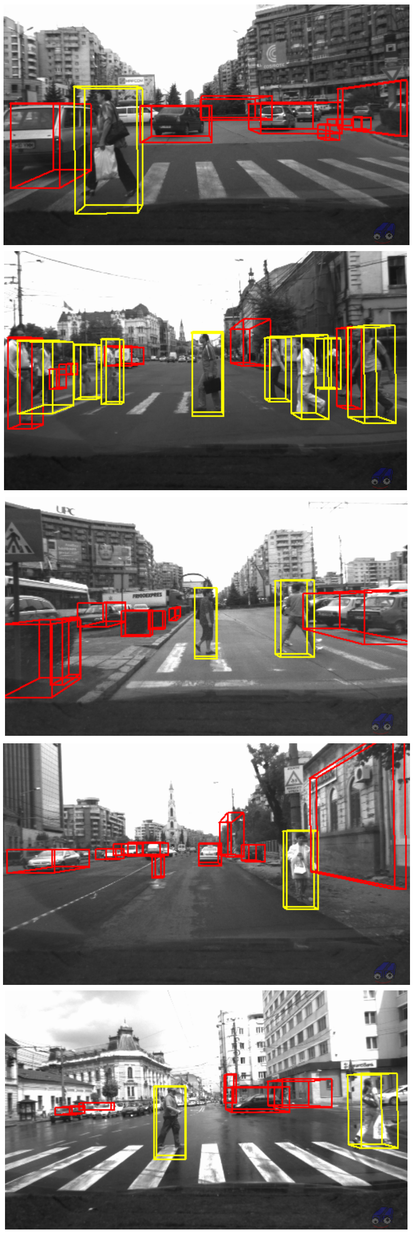

Figure 12: Classification results (pedestrians with yellow color; other obstacles with red color)

positive rate. This is very important for driving assistance systems because the driver shouldn't get false alarms or the vehicle must not automatically brake if there isn't truly a pedestrian. The results are comparable with the state of the art. In a stereo approach (Keller et al., 2011b) the authors achieve a detection rate of about 0.94 at 1 false positive per frame. In a monocular vision survey (Dollar et al., 2012) the best method achieves a detection rate of about 0.85 at 1 false positive per frame.

Although the true positive rate is not significantly improved (about 1.5%), there are situations in which a miss-detected pedestrian (by using a local matching dense stereo approach) is now correctly classified as being pedestrian. Samples of classification issues solved by improving the dense reconstruction with SORT-SGM are depicted in Figure 11: in the left image a traffic road sign was misclassified as pedestrian; in the right image the left-most pedestrian was misclassified as being other scene obstacle. Some classification final results are presented in Figure 12.

5. CONCLUSIONS

We developed a real-time stereo-vision pedestrian detection system that can be integrated as a module in a driving assistance system. The intensity scene points were acquired with two gray levels cameras and the depth was obtained using a software reconstruction with GPU (NVIDIA GeForce GTX 580) SORT-SGM algorithm. The quality and the number of reconstructed points are higher and more accurate than those obtained with a hardware stereo-reconstruction machine TYZX which uses a local matching approach.

We achieved better obstacle segmentation from background when using SORT-SGM algorithm instead of TYZX stereo-reconstruction, which leads to a more accurate features vector (based on both intensity and depth information). The introduced novel features (texture dissimilarity, humans' body specific features, distance related measures, speed) offer us a better pedestrian classification. All the features were used for training a robust random forest classifier model that can deal with feature missing values. In case of the obstacles that were successfully tracked across frames, a k-NN classification tracking method was used for filtering the spurious classification results that can appear for the same obstacle from frame to frame.

Our pedestrian detection system is performing in real-time (at about 25 fps) using the above mentioned GPU and an Intel Core 2 Duo E6750 processor.

A solution for future improvement of the current detection rate resides in the possibility of using color cameras for scene acquisition which brings more information, implementing a better reconstruction algorithm on GPU and extracting new features that will be combined for training a powerful classifier.

ACKNOWLEDGEMENTS

This paper was supported by the Romanian Agency of Scientific Research in the "Multi-scale multi-modal perception of dynamic 3D environments based on the fusion of dense stereo, dense optical flow and visual odometry information" project under Contract PN-II-ID-PCE-2011-3-1086.

REFERENCES

Benenson, R., Mathias, M., Timofte, R. & Van Gool, L. 2012. Pedestrian detection at 100 frames per second. *IEEE Conference on Computer Vision and Pattern Recognition (CVPR)*. pp. 2903-2910.

Bota, S. & Nedevschi, S. 2011a. Tracking multiple objects in urban traffic environments using dense stereo and optical flow. *14th International IEEE Conference on Intelligent Transportation Systems*. pp. 791-796.

Bota, S. & Nedevschi, S. 2011b. Vision based obstacle tracking in urban traffic environments. *IEEE International Conference on Intelligent Computer Communication and Processing (ICCP)*. pp. 231-238.

Bota, S., Nedevschi, S. & Konig, M. 2009. A framework for object detection, tracking and classification in urban traffic scenarios using stereovision. *IEEE 5th International Conference on Intelligent Computer Communication and Processing*. pp. 153-156.

Bregler, C. 1997. Learning and recognizing human dynamics in video sequences. *IEEE Computer Society Conference on Computer Vision and Pattern Recognition*. pp. 568-574.

Broggi, A., Bertozzi, M., Fascioli, A. & Sechi, M. 2000. Shape-based pedestrian detection. *IEEE Intelligent Vehicles Symposium*. pp. 215-220.

Dalal, N. & Triggs, B. 2005. Histograms of oriented gradients for human detection. *IEEE Computer Society Conference on Computer Vision and Pattern Recognition*. pp. 886-893 vol. 1.

Danescu, R., Nedevschi, S., Meinecke, M. M. & Graf, T. 2007. Stereovision Based Vehicle Tracking in Urban Traffic Environments. *Intelligent Transportation Systems Conference*. pp. 400-404.

Dollar, P., Wojek, C., Schiele, B. & Perona, P. 2012. Pedestrian Detection: An Evaluation of the State of the Art. *IEEE Transactions on Pattern Analysis and Machine Intelligence,* 34, pp. 743-761.

Elgammal, A., Duraiswami, R., Harwood, D. & Davis, L. S. 2002. Background and foreground modeling using nonparametric kernel density estimation for visual surveillance. *Proceedings of the IEEE,* 90, pp. 1151-1163.

Fardi, B., Schuenert, U. & Wanielik, G. 2005. Shape and motion-based pedestrian detection in infrared images: a multi sensor approach. *IEEE Intelligent Vehicles Symposium*. pp. 18-23.

Gandhi, T. & Trivedi, M. M. 2006. Pedestrian collision avoidance systems: a survey of computer vision based recent studies. *Intelligent Transportation Systems Conference*. pp. 976-981.

Gavrila, D. 2000. Pedestrian Detection from a Moving Vehicle. *Proceedings of the 6th European Conference on Computer Vision-Part II*, pp. 37-49.

Gavrila, D. M., Giebel, J. & Munder, S. 2004. Vision-based pedestrian detection: the PROTECTOR system. *IEEE Intelligent Vehicles Symposium*. pp. 13-18.

Gavrila, D. M. & Munder, S. 2007. Multi-cue Pedestrian Detection and Tracking from a Moving Vehicle. *International Journal of Computer Vision,* 73, pp. 41-59.

Gavrila, D. M. & Philomin, V. 1999. Real-time object detection for &ldquo;smart&rdquo; vehicles. *Proceedings of the Seventh IEEE International Conference on Computer Vision*. pp. 87-93 vol.1.

Giosan, I. & Nedevschi, S. 2009. Building Pedestrian Contour Hierarchies for Improving Detection in Traffic Scenes. *Proceedings of the International Conference on Computer Vision and Graphics: Revised Papers*, pp. 154-163.

Giosan, I., Nedevschi, S. & Bota, S. 2009. Real time stereo vision based pedestrian detection using full body contours. *IEEE 5th International Conference on Intelligent Computer Communication and Processing*. pp. 79-86.

Haller, I. & Nedevschi, S. 2010. GPU optimization of the SGM stereo algorithm. *IEEE International Conference on Intelligent Computer Communication and Processing (ICCP)*. pp. 197-202.

Haritaoglu, I., Harwood, D. & Davis, L. S. 2000. W4: real-time surveillance of people and their activities. *IEEE Transactions on Pattern Analysis and Machine Intelligence,* 22, pp. 809-830.

Havasi, L., Szlavik, Z. & Sziranyi, T. 2004. Pedestrian Detection Using Derived Third-Order Symmetry of Legs. *Proceedings of the IEEE International Conference on Computer Vision and Graphics*, pp. 11-17.

Hilario, C., Collado, J. M., Armingol, J. M. & Escalera, A. D. L. 2005. Pedestrian detection for intelligent vehicles based on active contour models and stereo vision. *Proceedings of the 10th international conference on Computer Aided Systems Theory*, pp. 537-542.

Javed, O. & Shah, M. 2002. Tracking and Object Classification for Automated Surveillance. *Proceedings of the 7th European Conference on Computer Vision-Part IV*, pp. 343-357.

Keller, C. G., Enzweiler, M. & Gavrila, D. M. 2011a. A new benchmark for stereo-based pedestrian detection. *IEEE Intelligent Vehicles Symposium (IV)*. pp. 691-696.

Keller, C. G., Enzweiler, M., Rohrbach, M., Fernandez Llorca, D., Schnorr, C. & Gavrila, D. M. 2011b. The Benefits of Dense Stereo for Pedestrian Detection. *IEEE Transactions on Intelligent Transportation Systems,* 12, pp. 1096-1106.

Khammari, A., Nashashibi, F., Abramson, Y. & Laurgeau, C. 2005. Vehicle detection combining gradient analysis and AdaBoost classification. *Proceedings of Intelligent Transportation Systems*. pp. 66-71.

Koller, D., Danilidis, K. & Nagel, H.-H. 1993. Model-based object tracking in monocular image sequences of road traffic scenes. *International Journal of Computer Vision,* 10, pp. 257-281.

Lipton, A. J., Fujiyoshi, H. & Patil, R. S. 1998. Moving target classification and tracking from real-time video. *Fourth IEEE Workshop on Applications of Computer Vision*. pp. 8-14.

Llorca, D. F., Sotelo, M. A., Hellín, A. M., Orellana, A., Gavilan, M., Daza, I. G. & Lorente, A. G. 2012. Stereo regions-of-interest selection for pedestrian protection: A survey. *Transportation research part C: emerging technologies,* 25, pp. 226-237.

Lun, Z., Li, S. Z., Xiaotong, Y. & Shiming, X. 2007. Real-time Object Classification in Video Surveillance Based on Appearance Learning. *IEEE Conference on Computer Vision and Pattern Recognition*. pp. 1-8.

Marita, T., Oniga, F., Nedevschi, S., Graf, T. & Schmidt, R. 2006. Camera Calibration Method for Far Range Stereovision Sensors Used in Vehicles. *IEEE Intelligent Vehicles Symposium*. pp. 356-363.

Masoud, O. & Papanikolopoulos, N. P. 2001. A novel method for tracking and counting pedestrians in real-time using a single camera. *IEEE Transactions on Vehicular Technology,* 50, pp. 1267-1278.

Nedevschi, S., Bota, S. & Tomiuc, C. 2009. Stereo-Based Pedestrian Detection for Collision-Avoidance Applications. *IEEE Transactions on Intelligent Transportation Systems,* 10, pp. 380-391.

Nedevschi, S., Danescu, R., Marita, T., Oniga, F., Pocol, C., Sobol, S., Tomiuc, C., Vancea, C., Meinecke, M. M., Graf, T., Thanh Binh, T. & Obojski, M. A. 2007. A Sensor for Urban Driving Assistance Systems Based on Dense Stereovision. *IEEE Intelligent Vehicles Symposium*. pp. 276-283.

Pantilie, C. D. & Nedevschi, S. 2012. SORT-SGM: Subpixel Optimized Real-Time Semiglobal Matching for Intelligent Vehicles. *IEEE Transactions on Vehicular Technology,* 61, pp. 1032-1042.

Papageorgiou, C. & Poggio, T. 2000. A Trainable System for Object Detection. *International Journal of Computer Vision,* 38, pp. 15-33.

Pocol, C., Nedevschi, S. & Obojski, M. A. 2007. Obstacle Detection for Mobile Robots, Using Dense Stereo Reconstruction. *IEEE International Conference on Intelligent Computer Communication and Processing*. pp. 127-132.

Rivlin, E., Rudzsky, M., Goldenberg, R., Bogomolov, U. & Lepchev, S. 2002. A real-time system for classification of moving objects. *16th International Conference on Pattern Recognition*. pp. 688-691 vol.3.

Rujikietgumjorn, S. & Collins, R. T. 2013. Optimized Pedestrian Detection for Multiple and Occluded People. *IEEE Conference on Computer Vision and Pattern Recognition*. pp. 3690-3697.

Stauffer, C. & Grimson, W. E. L. 2000. Learning patterns of activity using real-time tracking. *IEEE Transactions on Pattern Analysis and Machine Intelligence,* 22, pp. 747-757.

Toth, D. & Aach, T. 2003. Detection and recognition of moving objects using statistical motion detection and Fourier descriptors. *12th International Conference on Image Analysis and Processing*. pp. 430-435.

Woodlill, J. I., Gordon, G. & Buck, R. 2004. Tyzx DeepSea High Speed Stereo Vision System. *IEEE Conference on Computer Vision and Pattern Recognition Workshop*. pp. 41-41.